SURFACE DAMAGE MEASUREMENT TECHNIQUES FOR THE DETERMINATION OF FATIGUE CRACK INITIATION

B. C. Gowda* and H. R. Jhansale**

**Westinghouse Electric Corporation, Pittsburgh, PA, USA*
***Allis-Chalmers Corporation, Milwaukee, WI, USA*

ABSTRACT

In the present work a method based on a series of two level strain tests in which each axial specimen is strain cycled at an initial high strain amplitude for a specified number of cycles followed by low strain amplitude cycling to failure is described to delineate the two fatigue stages (I and II). The resulting initially overstrained long life fatigue behavior is analyzed with the aid of surface damage measurement techniques to estimate the durations of Stage 1 and Stage 11 crack growth periods.

KEY WORDS

Fatigue crack initiation, Stage I, crack growth, Stage II, Fracture, Over-strain, Surface damage, fatigue life.

INTRODUCTION

The nature of metal fatigue process is fairly well understood and the process is broadly divided into two periods, namely, a period of crack initiation and a period of crack propagation. However, the delineation between these stages, as first defined by Forsythe (1961), is yet to be standardized. Initial processes including bulk property changes such as cyclic hardening or softening and the formation of slip band intrusions and extrusions at the free surface belong to the stage of crack initiation. The stage at which the crack initiation process ends and the crack propagation process begins is very much a matter of opinion and judgement. Material scientists visualize an initiated crack size in terms of atomic scale, whereas engineers like to use a more readily observable macroscopic crack of thousandths of an inch or higher. Study of such small cracks has practical significance and benefit (Dowling, 1983).

It has also been accepted that it is appropriate to associate the completion of crack initiation to a physical change that occurs in the fatigue process, such as that occurring between stage I and stage II types of fatigue crack growth. Description of fatigue events in terms of these "stages" is now

generally accepted and their qualitative features are sufficiently well known. However, understanding the delineation of stage 1 and stage II crack growth processes is still developing. This paper presents a method of determining the stage I and stage II periods in a given fatigue life with the aid of surface damage measurement techniques.

Distinguishing Features of Stage I and Stage II

Stage I cracking, an extension of the slip band extrusion and intrusion process, grows along crystallographic planes closely oriented towards the planes of maximum resolved shear stress. With continued cyclic stressing, this shear mode cracking gives way to an open or tensile mode cracking called stage II and the crack growth now occurs macroscopically normal to the direction of the tensile stress. The depth and duration of stage I crack growth can vary to a large extent depending on several factors including the material, loading, environment and nature of stress state.

While low stress (or strain) levels favor continued stage I cracking, high stress levels encourage an early change over from stage I to stage II. In fact, in situations such as severe notched members and welds of average quality, local strains can be very high and cracks can grow in the stage II mode right from the start, apparently eliminating the stage I mode almost completely. Converse situations are also possible. Tensile mean stresses encourage stage II process. Thus, the higher the strain level and the higher the mean stress, the shorter is the duration of stage I crack growth at a given fatigue life.

Stage II fractographic studies and growth rate studies have been extensive (Feltner and Beardmore, 1970) and therefore are not included in this review.

AN APPROACH FOR DELINEATING STAGE I AND STAGE II CRACK GROWTH

Since it is known that stage I cracking generally occupies large fractions of life at low strain levels and small fractions of life at high strain levels, the life in a low strain amplitude test can be drastically reduced by a few initial cycles of a high strain amplitude (prestrain cycles). The effect of these prestrain cycles is to hasten stage I damage, and therefore a drastic reduction in life at the low strain level results (Watson and Topper, 1972). This phenomenon is best illustrated by means of an idealized schematic diagram as shown in Fig. 1. The number of prestrain cycles and the corresponding reduction in life at the low strain level are conveniently expressed as fractions of lives in constant amplitude tests at the corresponding strain levels. Thus, the prestrained long life damage for a two level strain test can be written in terms[1] of the Miner law:

$$N_1/N_{f1} = 1 - (N_2/N_{f2})$$

A plot of the quantities on left hand side and right hand side of the above equation is a straight line passing through the origin and having an angle of 45° with both axes. In cases where the Miner law is not valid, the above plot would yield a nonlinear relationship.

[1] The notations are defined in Table 1 if not defined in the text.

For the purpose of illustration, an idealized bilinear damage relationship is shown in Fig. 1. The initial steep slope of the bilinear curve represents the region of drastic life reduction and the shallower slope portion indicates the region of less drastic life reduction. Based on the foregoing argument regarding crack initiation and propagation periods, the "knee" in the bilinear plot of the overstrained long life behaviour delineates the stage I and stage II periods at both strain levels. It is interesting to note that bilinear representations of the type shown in Fig. 1 could also be used to study the nature of the cumulative damage law applicable to the material. In fact Manson (1967) proposed the "Double Linear Damage Rule" based on similar plots for several steels which closely approximated bilinear forms. A bilinear overstrain long life behavior is, in fact, a good relationship for several materials. In general, this relationship is influenced by the slip character and surface damage processes. In order to be able to determine the durations of stage I and stage II damage, therefore, the surface damage characteristics during the overstrained long life behaviour must be known.

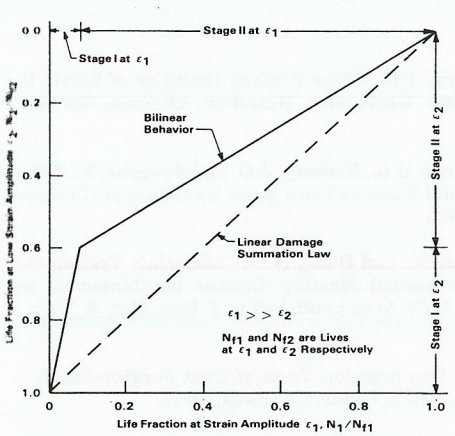

Fig. 1. Schematic of a Typical Overstrained Long Life Behavior Plot

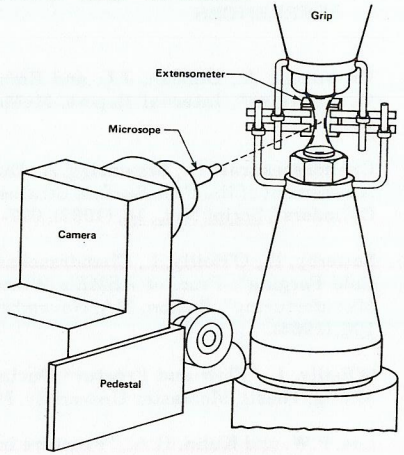

Fig. 2. Close Up View of Specimen Set Up

EXPERIMENTAL DETAILS

Material and Specimens

The material used was 0.5 inch diameter bar stock of Ferrovac 'E' iron, with 0.007 w/o carbon. Roughly machined axial specimens to be finally finished to the test section dimensions of 0.200 inch diamter and 0.30 inch gage length were annealed at 700°C for one hour in vacuum and then furnace cooled. Final machining was done by using successively lighter machining passes to minimize residual stresses. The test section surface was ground and then chemically polished.

Cyclic Straining/Stressing Procedure

All tests were performed using a closed loop system in fully reversed axial strain control. Strain was measured by means of a clip-on extensometer over the gage length of the specimen. The extensometer was mounted in the rear portion of the specimen in order to make the front half of the specimen surface available for microscopic observation during the test. A close-up view

of the specimen with the extensometer mounted on the rear side is shown in Fig. 2. The details of testing are similar to those in already published work (Abdel-Rauof, 1973; Chopra and Gowda, 1973).

The above quoted studies showed that the cyclic deformation and fatigue behavior of Ferrovac 'E' iron were strain rate sensitive even at room temperatures. Therefore a constant strain rate of .004 sec^{-1} was used in this study.

Definition of Life

In the strain controlled test the extensometer was programmed to cycle between two deformation limits, and therefore cyclic straining continued even after the specimens had partially fractured within the gage length. In the present invenstigation, fracture cycles were based on the stage at which the maximum load dropped rapidly towards zero in the load-time records.

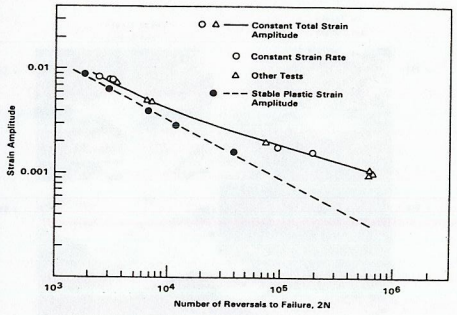

Fig. 3. Fatigure Life Curves for Ferrovac 'E' Iron

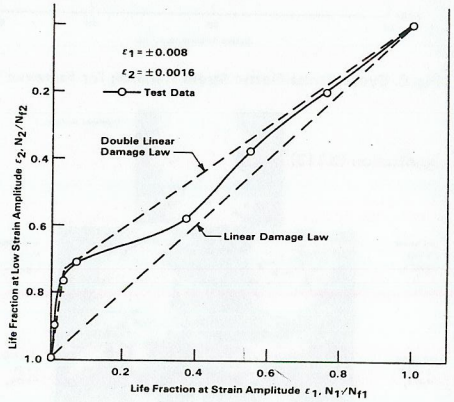

Fig. 4. Overstrained Long Life Behavior Plot for Ferrovac 'E' Iron (Total Strain-Life Criterion)

Constant Strain Amplitude Tests

These tests were used to generate the cyclic stress-strain and strain-life curves. Tests in which microscopic surface damage was periodically observed and recorded by surface micrograph methods required temporary interruptions to cycling. Comparison of fatigue lives between such interrupted and uninterrupted tests showed negligible difference in behavior between the two types of tests. Fig. 3 shows total strain amplitude (ϵ) vs. life data of both uninterrupted and interrupted tests. As the tests were in total strain amplitude control, stable plastic strain amplitude values were used in generating this plot.

Two Block Tests

Each test consisted of a specified number of cycles at a higher strain (ϵ_1) amplitude of $\pm$ 0.008 followed by a lower strain (ϵ_2) amplitude of $\pm$ 0.0016 (nominal) for the rest of the life. The transfer from the higher to the lower strain level was achieved by first unloading along the elastic line to zero

strain from a point on the loading branch of the hysteresis loop and then restarting the test in tension at the low strain level.

Thus, in each test while the two levels of strain amplitudes were approximately the same, the number of prestrain cycles varied from test to test. A normalizing procedure for life determination was used to account for the small variations (see Table 1) in the strain levels.

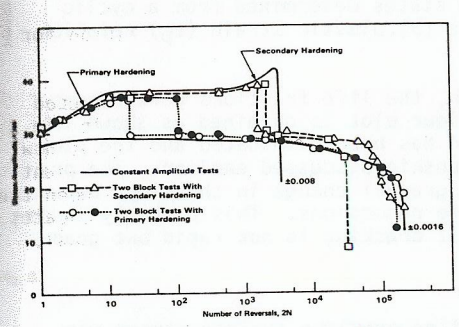

Fig. 5 Cyclic Stress Respone of Ferrovac 'E' Iron

Table 1. Two Block Test Data and Life Fraction Calculations

Test	ϵ_1	N_1	N_{f1}	ϵ_2	N_2	N_{f2}	σ_2	ϵ_p	N_{fp2}	N_1/N_{f1}	N_2/N_{f2}	N_2/N_{fp2}
1	± 0.008	10	1350	± 0.00152	85000	95000	27.5	0.0006	100000	.0076	0.89	.85
2	± 0.008	50	1350	± 0.00155	67500	85000	27.7	0.00063	90000	.037	.76	.74
3	± 0.008	100	1350	± 0.00152	67500	95000	27.5	0.0006	100000	.076	.71	.67
4	± 0.008	500	1350	± 0.00152	54500	95000	30.6	0.00052	130000	.37	.57	.42
5	± 0.008	750	1350	± 0.00155	32750	85000	30.0	0.00055	115000	.56	.39	.28
6	± 0.008	1000	1350	± 0.0016	15200	75000	30.0	0.0006	100000	.76	.20	.15

Notations:

$\epsilon_p = \epsilon_2 - (\sigma_2/E)$; $E = 30 \times 10^3$ k.s.i.

σ_2 = Stress amplitude (k.s.i.) at ϵ_2 strain amplitude

N_1, N_2 = Number of cycles at strain amplitude ϵ_1, ϵ_2, respectively

N_{f1}, N_{f2} = Number of cycles to failure at ϵ_1, ϵ_2 based on total strain life criterion, respectively

N_{fp2} = Number of cycles to failure at ϵ_2 based on plastic strain life criterion

ANALYSIS OF RESULTS

Analysis of Overstrained Long Life Behavior of Ferrovac 'E' Iron

Overstrained long life data for Ferrovac 'E' iron obtained from two block tests are shown in Fig. 4. While this plot is generally in agreement with the typical characteristics illustrated in Fig. 1, there is a peculiar dip in the curve, suggesting an apparent tendency for improvement in predicted life if the double linear damage criterion is used. An inspection of the stress response behaviour during these tests suggested a possible cause for this peculiar behaviour, which is explained below.

Influence of Cyclic Stress Response

Figure 5 shows a comparison of the cyclic stress response between the three types of tests. At the high strain amplitude Ferrovac 'E' iron exhibits two hardening stages, the initial one being a common feature of annealed metals, but the later one peculiar to this material. This secondary hardening also observed in an earlier investigation (Abdel Rauof, 1973) has been attributed to the dynamic strain aging property of the material. At the low strain amplitude, there is little or no apparent hardening initially, but a gradual softening. It is interesting to note that in those two block tests where the prestrain cycles were not sufficient to reach the secondary hardening stage, the stress response at the subsequent low strain amplitude closely follows that of the constant strain amplitude test. This indicates that the plastic strain amplitude in these tests remains the same. Since the total strain and stress is the same in each of the tests, the plastic strain should also be the same. However, in those two block tests where the prestrain cycles induce secondary hardening, the stress response at the low strain amplitude is notably higher than that in the constant strain amplitude test indicating that the plastic strain amplitude is lower in two-block tests than that in the constant strain amplitude tests (Fig. 3). Now, if life fractions are based on plastic strain vs. life criterion instead of a total strain vs life criterion

as done earlier in generating Fig. 4, the apparent dip observed in the figure can be explained.

Plastic Strain Basis for Life Fractions

The fatigue data reported is generated using constant total strain control rather than constant plastic strain control. However, an approximate plastic strain-life curve was generated (see Fig. 3) on the basis of plastic strain amplitudes corresponding to the stable states determined from a cyclic stress-strain curve. The cyclic stress (σ), plastic strain (ε_p) relation for Ferrovac 'E' is shown in Fig. 6.

Using the plastic strain-life criterion, the life fractions were recomputed and a new overstrained long life behaviour plot is obtained as shown in Fig. 7. The peculiar dip observed in Fig. 4 has been eliminated and the plot now is more typical of the bilinear relationship discussed earlier. The present curve of the plotted results do show a gradual change in the slope between the regions of drastic and less drastic life reductions. This probably indicates that the change from stage I to stage II cracking is not rapid but gradual.

Surface Damage Observations

Simultaneous with the fatigue life testing, specimen surface damage was recorded by means of an optical microscope with a camera attachment. The objective of this effort was to investigate the feasibility of making direct observations at as high a magnification as possible and to quanitify surface damage and seek damage correlations with the various stages in life. Equipment and set-up limitations allowed observations and recording of reasonably good pictures up to magnifications of 400. At this magnification microscopic damages of the transgranular and intergranular variety can be easily distinguished and studied. Some scanning electron microscopic pictures of the surface damage at failure were also taken. Concentrated and extensive future effort is suggested in this direction. Replication of surface damage at various life fractions is another useful technique under pursuit but not reported here.

In Fig. 8 surface damages at the low and high strain levels are compared at approximately the same fractions of life. Figure 9 compares fracture surfaces between the low and the high strain levels at three magnifications. Surface damage in the form of slip striations are apparent at both strain levels as early as 1 percent of life. At low strains slip lines are concentrated near defects, triple points and grain boundaries. At high strains the slip lines are more or less homogeneously distributed and extend across grain boundaries, whereas at low strains they terminate at grain boundaries or within grains. At both low and high strains slip lines appear as parallel bands increasing in number and deepening as grooves with continued cycles. During the early part of life very little criss-crossing of slip lines is present both at low and high strain cycles. But during the later stages of life criss-crossing develops only in the case of high strain cycles. Damage at low strains is localized and quite a number of grains virtually undamaged. Triple points and grain boundaries are the most vulnerable sites of this localized damage.

Surface damage at the time of fracture are compared between constant strain and two step tests in Fig. 10. Specimens which had a small number of initially high strain cycles (up to 10 percent of life) followed by low strain cycles exhibit surface damage characteristics of low strain amplitude tests.

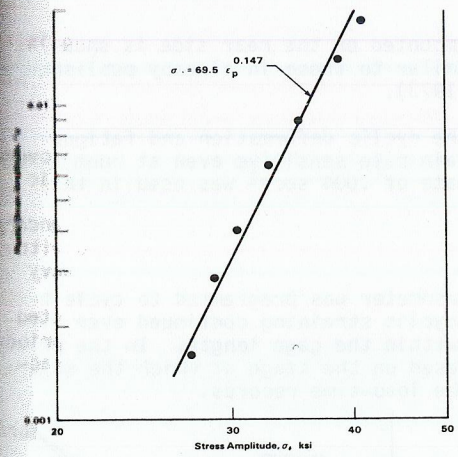

Fig. 6. Cyclic Stress-Plastic Strain Relation for Ferrovac 'E'

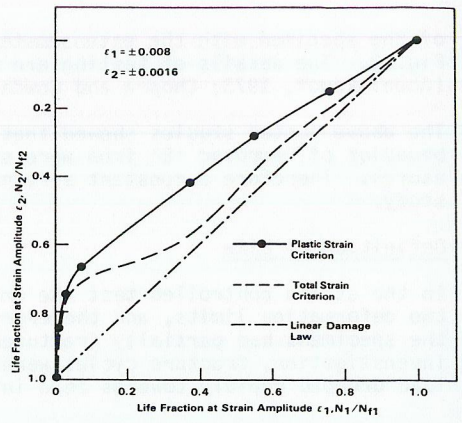

Fig. 7. Overstrained Long Life Behavior Plot for Ferrovac 'E' Iron (Plastic Strain-Life Criterion)

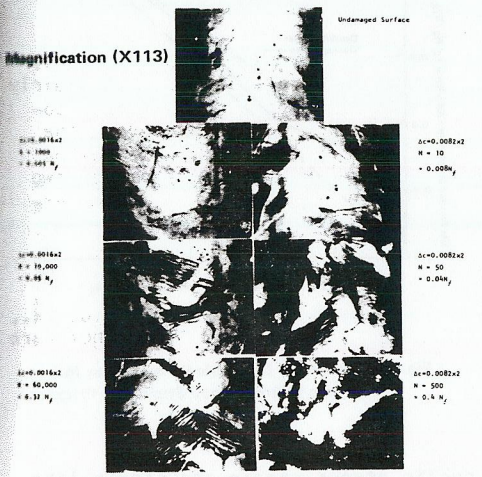

Fig. 8. Optical Micrographs Showing Progressive Surface Damage in Low and High Strain Cycling

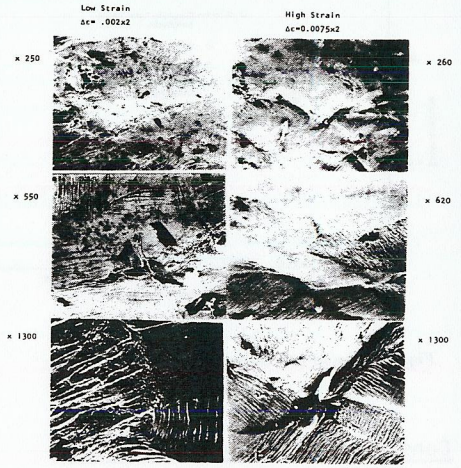

Fig. 9. Scanning Electron Micrographs Showing Surface Damage at Fracture in Low and High Strain Fratigure Tests

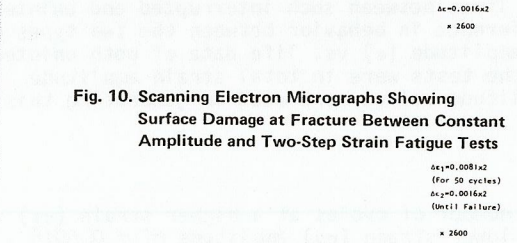

Fig. 10. Scanning Electron Micrographs Showing Surface Damage at Fracture Between Constant Amplitude and Two-Step Strain Fatigue Tests

The criss-crossing of slip lines if developed during high strain cycling is not affected by the subsequent low strain cycling.

DISCUSSION AND CONCLUSIONS

In general, the effect of the prior history dependent stress response on overstrained long life behavior can be accounted for by considering the plastic strain-life instead of the total strain-life criterion. The property of stress dependence on prior history caused in this case by the unique secondary hardening is also exhibited by more common structural metals associated with planar slip character (Feltner and Beardmore, 1967). Pure metals with wavy slip character are generally believed to exhibit a unique stable stress response independent of prior history. But even these metals, when subjected to two block strains of widely different levels, a stress dependence on prior history results. Thus a plastic strain criterion for calculating life fractions becomes a necessary part of the analysis.

Surface damage observations showed that stage I cracking is predominantly surface grooving and a localized high strain level accelerates this process. Other factors influencing the overstrained long life fatigue behaviour did not significantly affect the stage I and stage II calculations for Ferrovac 'E' iron.

The approach discussed for determining the durations of stage I and stage II in life has an attractive feature in that the measurements involved are fairly simple and direct as compared to those required in a ripple counting fractographic approach or other approaches. However, it should be noted that the method is an indirect approach and needs further work. More surface damage correlations through micrographic and replica techniques, other forms of two step tests with different combinations of strain levels and different materials will help to confirm the usefulness of this approach.

ACKNOWLEDGEMENTS

Financial support for this work was from the N.R.C. of Canada, and A.F.O.S.R., USA. The work was carried out at the University of Waterloo. The authors are grateful to Prof. T. H. Topper for his encouragement and guidance.

REFERENCES

Abdel-Raouf, H.A. Plumtree, and T.H. Topper (1973). Effects of Temperature and Deformation Rate on Cyclic Strength and Fracture of Low Carbon Steel, A.S.T.M. STP 519.

Chopra, O.K., and B.C. Gowda (1973). Substructural Changes During Cyclic Deformation of α-Iron, Philosophical Magazine.

Dowling, N.E. (1983). Growth of Short Fatigue Cracks in an Alloy Steel, SAE Trans.

Feltner, C.E., and C. Laird (1967). Cyclic Stress-strain Response of F.C.C. Metals and Alloys, ACTA Metallurgica 15.

Feltner, C.E., and P. Beardmore (1970). Strengthening Mechanisms in Fatigue, A.S.T.M. special tech. publ. 467.

Forsyth, P.J.E. (1961). A Two Stage Process of Fatigue Crack Growth, Proc. Crack Propagation Symposium, Cranfield, September 1961.

Manson, S.S., J.R. Freche, and C.R. Ensigh (1967). Application of a Double Linear Damage Rule to Cumulative Fatigue, A.S.T.M. STP 415.

Watson, P., and T.H. Topper (1972). Fatigue Damage Evaluation for Mild Steel Incorporating Mean Stress and Overload Effects, Exp. Mech. 12.